Presented at the International Daylighting
Conference, Phoenix, AZ, February 16-18, 1983;
and to be published in Energy and Buildings

PHOTO-ELECTRIC CONTROL OF EQUI-ILLUMINATION
LIGHTING SYSTEMS

F.M. Rubinstein

April 1983

PHOTO-ELECTRIC CONTROL OF EQUI-ILLUMINATION LIGHTING SYSTEMS

F. M. Rubinstein

Lighting Systems Research Group
Lawrence Berkeley Laboratory
University of California
Berkeley, CA 94720   U.S.A.

April 1983

PHOTO-ELECTRIC CONTROL OF EQUI-ILLUMINATION LIGHTING SYSTEMS

Francis Rubinstein
Energy Efficient Buildings Program
Lawrence Berkeley Laboratory
University of California
Berkeley CA   94720   USA

ABSTRACT

The ability of a photo-electrically controlled lighting system to maintain a constant light level on a task surface by responding to changing daylight levels is affected by the control algorithm used to relate the photosensor signal to electric light levels and by the geometry and location of the photosensor. We describe the major components of a typical equi-illumination system, discuss the design and operation of such a system, and examine the effects of the control algorithm and photosensor shielding. Equations for the control photosensor signal are developed that separate the signal into electric light and daylight components. We then present mathematical descriptions for the constant set-point control algorithm used by most manufacturers. An alternative, sliding set-point algorithm is proposed in which the total photosensor signal is a linear function of the signal's daylight component. Computer simulations of the performance of dimmable lighting control systems driven by ceiling-mounted photosensors were run for a test room under various daylight conditions. Control systems using the constant set-point algorithm were unable to provide the target light level continuously, although shielding the ceiling-mounted photosensor from the window luminance resulted in higher maintained levels with less variability than did using unshielded photosensors. The use of a sliding set-point algorithm in lieu of a constant set-point algorithm improved the performance of systems driven by both shielded and unshielded photosensors. When a sliding set-point

system was used in conjunction with a photosensor shielded from the window, a nearly constant light level was maintained at the task surface regardless of daylight condition.

INTRODUCTION

A major purpose of a lighting control system is to provide suitable levels of illumination for the performance of visual tasks while minimizing electrical energy consumption. The potential of such systems to reduce lighting energy use in daylighted buildings has been documented [1,2,3]. In areas near windows and skylights, an ideal equi-illumination system would supplement the available daylight on the task area with just enough electric lighting to meet the design level. Because daylight is a continually changing quantity, an equi-illumination lighting system must use a control photosensor to continually sample ambient light levels in the controlled building space. Furthermore, the system must use some built-in control algorithm to determine exactly how much electric light to supply based on the signal from the control photosensor. In principle, the objective of constant illuminance at the task surface can be achieved by placing a cosine-corrected control photosensor on the work surface and using a control algorithm that continually adjusts electric light levels to keep a constant total light level on the photosensor (and therefore the task). Although this scheme fulfills the requirement of equi-illumination at the work surface, it is undesirable to place the control photosensor at the workplane due to the confounding effects of light-obstructing objects (body shadows, loose papers, etc.). Instead the photosensor is mounted elsewhere, often in the ceiling pointing down [4]. Maintaining a constant light level on the task then becomes more complex because a given change in relative photosensor signal may not cause the same change in task illuminance for both daylight and electric light. The work presented here examines how the control algorithm and the photosensor's geometry and location affect the ability of a photo-electrically controlled lighting system to maintain a constant light level

at the task by responding to changes in daylight levels.

DESIGN AND OPERATION OF PHOTO-ELECTRICALLY CONTROLLED LIGHTING SYSTEMS

The ability of a photo-electric control system to provide a constant light level on a task surface can be determined by mathematically analyzing the relationships among the various system components and the luminances within the building space. Below we describe the components of a typical photo-electric control system and then derive expressions that characterize the operation of the system under various daylight conditions. Based on this analysis, we can determine the total illuminance delivered to the task surface for various control systems.

System components

A photo-electrically controlled lighting system consists of three basic components:

1) a control photosensor that generates an electrical signal proportional to the amount of light impinging on its surface;

2) a logic circuit that incorporates a control algorithm to process the photosensor's signal and convert it to a control signal for a dimming unit;

3) a dimming unit that smoothly varies the electric light output by altering the amount of power flowing to the lamps.

While there are many commercially available systems, ranging from large units that simultaneously dim entire banks of lights, to high-frequency ballasted systems capable of controlling individual fixtures, all dimming systems incorporate the above elements in some fashion. This discussion is limited to dimmable fluorescent systems because

fluorescent lighting dominates in commercial and industrial buildings and is the only commercial light source that can be dimmed efficiently over a large dynamic range with minimal shifts in spectral distribution. Figure 1 is a simplified graphic representation of how these system elements are typically integrated into a building space. The ceiling-mounted photosensor links the ambient light levels in the space (both daylight and electric) to the logic circuit, which, in turn, adjusts the electric light output according to a built-in control algorithm. Thus the design of the control photosensor and the logic circuit and the interaction of these two elements largely determine the lighting conditions in the building space.

Control photosensor

The control photosensor typically consists of a silicon photodiode in a housing. The housing's geometry determines the photodiode's sensitivity to light from different directions. In order for the control photosensor to evaluate the spectral content of the measured light in the same manner as the human eye, the photosensor should incorporate a color-correcting (photopic) filter. Finally, to insure that the signal generated by the sensor is proportional to the light impinging on its surface, the photo-diode usually is connected to an operational amplifier operated in the transimpedance mode. With such a circuit, the output voltage S(t) of the operational amplifier is proportional over a large range to the light falling on the photodiode. For a color-corrected photosensor, we can write an expression for the control photosensor signal $S_T(t)$:

$$S_T(t) = \int L_T(\Omega, t) R(\Omega) d\Omega, \tag{1}$$

where $L_T(\Omega, t)$ is the spatial luminance distribution in the room from both

daylight and electric light at time t; R(Ω) is the spatial responsivity of the control photosensor; and Ω is the solid angle over which the integral is performed. For the circuit configuration described previously, $L_T(\Omega,t)$ has units of $cd\ m^{-2}$, and R(Ω) is in $volts\ m^2cd^{-1}sr^{-1}$.

To conveniently evaluate the behavior of systems in which the control photosensor's location is such that both daylight and (controlled) electric light are sensed, one can separate the $L_T(\Omega,t)$ in Eq. (1) into a daylight component $L_D(\Omega,t)$ and an electric light component $L_E(\Omega,t)$:

$$S_T(t) = \int L_D(\Omega,t)R(\Omega)d\Omega + \int L_E(\Omega,t)R(\Omega)d\Omega. \tag{2}$$

The first term in Eq. (2) is that portion of the total photosensor signal attributable to daylight alone; the second term is that portion from electric light. To simplify the nomenclature, we introduce $S_D(t)$ and $S_E(t)$, which are defined to be the first and second terms, respectively, in Eq. (2). That is:

$$S_T(t) = S_D(t) + S_E(t). \tag{3}$$

If we assume that all the electric lights dim uniformly with respect to one another, then the second term in Eq. (2) or (3) can be simplified by writing the luminance distribution of the electric light as the product of a time-dependent function and a time-independent constant as follows:

$$L_E(\Omega,t) \equiv \delta(t)L_{E_{max}}(\Omega) \tag{4}$$

and

$$S_E(t) = \delta(t)\int L_{E_{max}}(\Omega)R(\Omega)d\Omega, \tag{5}$$

where $L_{E_{max}}(\Omega)$ is the luminance distribution of the electric lighting

system at 100% light output and $\delta(t)$ is the fractional dimming level, assumed to run between 0 and 1. The integrand in Eq. (5) is time-independent and integrates to a constant $S_{E_{max}}$, which is simply the photosensor voltage generated when the photosensor is exposed to only electric light at full intensity. Equations (3) and (5) can be combined to yield an expression that relates the fractional dimming level $\delta(t)$ to the total signal generated by the control photosensor, $S_T(t)$, and to that fraction of photosensor signal attributable only to daylight, $S_D(t)$:

$$\delta(t) = \frac{S_T(t) - S_D(t)}{S_{E_{max}}}. \qquad (6)$$

Control algorithms for the logic circuit

The logic circuit determines how much electric light to supply by using a control algorithm to process the signal $S_T(t)$ from the control photosensor. The purpose of the control algorithm is therefore to fix the relationship between the various terms in Eq. (6). Clearly the algorithm employed by the control system is of crucial importance to achieving constant illumination at the work plane. The choice of control algorithm is left to the manufacturer of the logic circuit. Typically, the simpler the form of the algorithm, the simpler it is to design and operate the system. A survey of commercially available photo-electric dimming systems indicates that most manufacturers employ the simplest possible control algorithm, which here is termed the constant set-point algorithm.

Constant set-point algorithm

A control system that uses the constant set-point algorithm will continually adjust the fractional dimming level of the electric lighting so that the control photosensor signal is maintained at a constant, pre-set

level. In practice, the level of photosensor signal to be maintained is nearly always set by operating the electric lights at full intensity at night, measuring the voltage generated and adjusting a reference circuit in the logic circuit so as to establish that voltage as the set-point voltage. (This process of determining and setting the set-point level at the installation site is referred to as "calibrating" the dimming system.) Then, during daytime operation, as the daylight level in the space increases, the control photosensor signal will tend to exceed the set-point level, causing the electric lighting system to dim until the photosensor signal once again equals the set-point voltage. In systems incorporating this control algorithm,

$$S_T(t) = S_{E_{\max}},\qquad\qquad\qquad\qquad\qquad\qquad (7)$$

where $S_{E_{\max}}$ is the voltage produced by the control photosensor when exposed to full electric light but no daylight. Using Eqs. (6) and (7), we obtain

$$\delta(t) = 1 - \frac{S_D(t)}{S_{E_{\max}}} \qquad 0 \le S_D(t) \le S_{E_{\max}}, \qquad\qquad (8a)$$

which gives the fractional dimming level as a function of the independent parameter $S_D(t)$, which is that part of the total photosensor signal attributable to daylight alone. Equation (8a) holds for only the range of $S_D(t)$ indicated. Once the daylight component exceeds $S_{E_{\max}}$, the control system will turn off the electric lighting:

$$\delta(t) = 0 \qquad S_D(t) > S_{E_{\max}}. \qquad\qquad\qquad\qquad (8b)$$

Because we are interested in the illuminance on the work plane, we need an expression relating Eq. (8a) to the daylight illuminance at the

work plane, $I_D(t)$, and the electric light level, $I_E(t)$:

$$I_T(t) = I_D(t) + I_E(t) \tag{9}$$

and

$$I_E(t) = \delta'(t)I_{E_{\max}}, \tag{10}$$

where $I_T(t)$ is the total light level and $I_{E_{\max}}$ is the maximum electric light level at the work plane. For the $\delta'(t)$ in Eq. (10) to be identical to the $\delta(t)$ in Eq. (6) implies that

$$\frac{I_E(t)}{I_{E_{\max}}} = \frac{S_E(t)}{S_{E_{\max}}}, \tag{11}$$

which is reasonable for a uniformly dimming lighting system because the relative spatial distribution of electric lighting in the room should be constant regardless of the dimming level. Combining Eqs. (8)-(10) gives the total illuminance on the work plane:

$$I_T(t) = I_D(t) + I_{E_{\max}}\left[1 - \frac{S_D(t)}{S_{E_{\max}}}\right] \qquad 0 \le S_D(t) \le S_{E_{\max}} \tag{12a}$$

$$I_T(t) = I_D(t) \qquad S_D(t) \ge S_{E_{\max}} \tag{12b}$$

for a lighting control system that employs the constant set-point algorithm. Equation (12) allows one to calculate the total light level on the task for a constant set-point system given values of $I_D(t)$ and $S_D(t)$ for the photosensor configuration of interest. A simple study, described in the Experimental Objective and Method section, was undertaken to empirically measure $S_D(t)$ and $I_D(t)$ for a selected set of photosensors under

real sky conditions.

It is informative to examine the way Eq. 12 constrains the possible ratios of $I_D(t)$ to $S_D(t)$ if the control photosensor is to maintain constant illuminance on the work plane. To do this, one sets the right side of Eq. (12a) equal to the design lighting level, $I_{E_{\max}}$, and solves for $S_D(t)/I_D(t)$;

$$\frac{S_D(t)}{I_D(t)} = \frac{S_{E_{\max}}}{I_{E_{\max}}}. \tag{13}$$

A constant set-point system will therefore maintain a constant light level at the task if and only if the control photosensor can satisfy the relationship expressed in Eq. 13. Because the left side of Eq. 13 is determined solely by the *daylight* luminance distribution within the room, while the right side is a function only of the *electric* light luminance distribution, there is no physical requirement that any photosensor will satisfy Eq. 13 in the general case (except for the trivial situation in which the control photosensor is mounted on the task surface).

The constraints imposed by Eq. 13 are a direct consequence of the constant set-point algorithm, which requires that $S_T(t) = S_{E_{\max}}$. Although this is the simplest way for a control system to fix the relationship between the photosensor signal and the electric light level, it is possible to design control systems that use different algorithms possibly better suited to maintaining a constant light level at the task.

Sliding set-point algorithm

This section describes an alternative control algorithm that can be incorporated into a dimmable lighting control system to keep the total illumination on the work plane constant at least to the extent that $S_D(t)/I_D(t)$ is constant with time. Unlike the constant set-point

algorithm in which S_T = constant, the sliding set-point algorithm uses:

$$S_T(t) = (1-M) S_D(t) + C, \tag{14}$$

where $1-M$ and C are constants. A control system that uses this algorithm will adjust the fractional dimming level $\delta(t)$ so that the total photosensor signal is a linear function of $S_D(t)$. By calibrating the system at night as previously described, the value of C is determined from the boundary condition that S_T at night should equal $S_{E_{max}}$:

$$S_T(t) = (1-M) S_D(t) + S_{E_{max}}. \tag{15}$$

To fix the value of $1-M$ in a particular installation, one need simply adjust the fractional dimming level $\delta(t)$ so that the total illuminance at the work plane at some time during the day, t_{cal}, matches the design lighting level, $I_{E_{max}}$. Using Eqs. (9) and (10):

$$I_T(t_{cal}) = I_{E_{max}} = I_D(t_{cal}) + \delta(t_{cal}) I_{E_{max}}. \tag{16}$$

Given Eqs. (6), (15), and (16) one can solve for M:

$$M = \frac{S_{E_{max}} / I_{E_{max}}}{S_D(t_{cal}) / I_D(t_{cal})}. \tag{17}$$

Using Eqs. (6), (9), (10), and (15) we obtain an expression for the total illuminance on the work plane:

$$I_T(t) = I_D(t) + I_{E_{max}} \left[1 - M \frac{S_D(t)}{S_{E_{max}}} \right] \qquad 0 \le S_D(t) \le \frac{S_{E_{max}}}{M} \tag{18a}$$

$$I_T(t) = I_D(t) \qquad S_D(t) > \frac{S_{E_{max}}}{M}. \tag{18b}$$

where M is as given in Eq. (17). From Eqs. 18a and 18b we can determine the total light level on the task for a sliding set-point system given values of $I_D(t)$ and $S_D(t)$ for a particular photosensor.

To obtain a constant illuminance on the work plane, the right side of Eq. (18a) must equal $I_{E_{max}}$ for all values of t. That is:

$$\frac{S_D(t)}{I_D(t)} = \frac{S_D(t_{cal})}{I_D(t_{cal})} . \tag{19}$$

If Eq. (19) is not satisfied for a photo-electric dimming system employing the sliding set-point algorithm, then a constant level of light will not be maintained on the work plane. For this kind of system, it is clear that the extent to which equi-illumination is achieved depends, first, on whether $I_D(t)$ is strictly proportional to $S_D(t)$ for various daylight conditions, and, second, on the extent to which $S_D(t_{cal})/I_D(t_{cal})$ approximates the more general ratio $S_D(t)/I_D(t)$. Note that if Eq. (13) is satisfied for a fortuitously configured photosensor, then M in Eq. (17) becomes unity and Eq. (18a) reduces to Eq. (12a) as expected. For the general case, however, where $S_{E_{max}}/I_{E_{max}}$ is not equal to $S_D(t)/I_D(t)$, the ability to adjust the value of M with the sliding set-point algorithm enables a user to adjust the lighting system's response to compensate for the inequality of these two ratios.

EXPERIMENTAL OBJECTIVE AND METHOD

The objective of the experiment reported here was to obtain simultaneous measurements of $S_D(t)$ and $I_D(t)$ for various photosensors in a typical daylighted room in order to examine the ability of constant and sliding set-point systems to maintain equi-illumination at the task

surface. Light levels were measured under various conditions in a test room that had ceiling-mounted photosensors aimed at selected room surfaces and a photometer located on the task surface.

The test room (southwest-facing) measured 4.6 m by 4.6 m with a ceiling 2.7 m high (15 ft x 15 ft x 9 ft) and had a single window (clear 88% transmissive) fitted with movable drapes (approximately 15% transmissive). The window-to-wall ratio was 43%. Seven photometers, especially modified to mimic the performance of typical control photosensors, were attached at the ceiling center point and aimed at strategic locations in the room. Four of these photometers were fitted with opaque black cylindrical shrouds that restricted the field of view to a cone of 20-degree semi-angle. Each of the four photosensors was aimed at the center point of one wall so that it was sensitive only to the light reflected from that wall. These four photometers therefore measured a physical quantity that was closely related to but not exactly equivalent to the *average wall luminance*. These are referred to as the P_{NE}, P_{SE}, P_{SW}, and P_{NW} photosensors, the subscript denoting the direction at which the photosensor was aimed. The remaining three photosensors in the ceiling cluster, P_{tl}, P_{ce}, and P_{ces}, were mounted flat to the ceiling surface and thus pointed straight down at the center point of the floor. Photosensor P_{tl}, equipped with an opaque shroud that restricted its field of view to a cone of 40-degree semi-angle, was used to measure (or at least approximate) the average luminance of the task surface and surrounding floor below. The two remaining photosensors were both cosine-corrected; P_{ces} was equipped with an opaque baffle to shield it from direct light from the window. The last photosensor in the ceiling cluster, P_{ce}, having no baffle or shield, simply measured the *illuminance at the center of the ceiling*. The daylight on the task surface was measured by another cosine-corrected

photometer.

Measurements were taken in the southwest room under clear sky conditions. With the electric lights off, all photometers (photosensors) were read simultaneously at 30-minute intervals throughout the day with the room drapes open and then closed. Each measurement therefore yielded the $S_D(t)$ and the corresponding value of $I_D(t)$ for each photosensor. The photosensors were also read once at night with the electric lights on to establish the values of $S_{E_{max}}$ and $I_{E_{max}}$.

RESULTS

To examine the relationship between $S_D(t)$ and $I_D(t)$ for each of the tested photosensors, first the data for each were disaggregated into two data sets according to drape position (open or closed); then each data subset was fitted to a single parameter B in:

$$I_D / I_{E_{max}} = B \ S_D / S_{E_{max}} \qquad (20)$$

using the least-squares method. Because Eq. (20) is simply the generalized form of Eqs. (13) and (19), fitting the data to Eq. (20) allows us to test the validity of these equations. Table 1 lists the calculated values of B for each photosensor and drape condition and also shows the statistical uncertainties in our estimates of B. The uncertainty, σ_B, and the correlation coefficient, r, are useful for evaluating the performance of a particular photosensor; if a photosensor has a small value of σ_B relative to B and an r close to 1, we conclude that the relationship between $S_D(t)$ and $I_D(t)$ is close to simple *proportionality*. Note that data points for which $I_D(t)$ was much larger than the design level (i.e., 50% greater) were excluded

from the fits shown in Table 1 because one may assume that at these high light levels the electric lights would be off.

Although the quantity of data collected in this study was small, the results shown in Table 1 illustrate an important point: none of the photosensors tested was able to satisfy Eq. 13, which requires that the fitted parameter B in Eq. (20) be equal to unity. In fact, the values of B calculated for all the photosensors are consistently less than one: the P_{ces}, P_{SE}, and P_{tl} photosensors all had B roughly equal to 0.7, while the remaining photosensors had significantly smaller values of B. To better understand the implications of these data with respect to the objective of equi-illumination, a simulation program was written to compute the task illuminance levels using the measured data as input. The simulation results for two photosensors, P_{ces} and P_{ce}, are presented in the following section. These photosensors were selected because they represent the range of B encountered in this study, i.e., a relatively high B for the P_{ces} sensor and a low B for P_{ce}.

Constant set-point systems

The performance of a photo-electrically controlled lighting system driven by each of the photosensors in the ceiling cluster was evaluated by computer simulation. To simulate the performance of systems employing the constant set-point algorithm, the light levels on the task surface were computed using Eqs. (12a) and (12b). The computer model incorporated the assumption that the electric lighting system in the test rooms was entirely direct and could be dimmed uniformly from 100 to 0%. Selected results from these simulations for drapes closed conditions are shown in Figs. 2 and 3. The relative contribution of daylight to the total illumination level on the task surface reached a maximum (750 lux) at

2:00 pm, exceeding the target level by 150 lux. The target level is the task illumination level measured at night with the electric lights at maximum (i.e., 591 lux). An equi-illumination system would supplement the daylight with sufficient electric light to raise the total to the target level except between 1:00 and 2:30 pm, when no electric light would be supplied because daylight would exceed the target level.

Figure 2 shows the maintained light levels for a photo-electrically controlled system employing the constant set-point algorithm and driven by the ceiling illuminance photosensor P_{ce}. The system performed poorly, producing large variations in total light level at the task. Between 10:30 am and 1:00 pm and between 2:30 and 3:30 pm, this lighting system would supply no electric illumination although the daylight component was much less than the target level. At 10:30 am, the total light level was only one-sixth of the target level.

Figure 3 shows the performance of a dimming system driven by the P_{ces} photosensor, which was shielded to prevent it from directly detecting the window luminance. This system performed better than the unshielded photosensor system, as evidenced by the lesser illuminance variability and the generally higher maintained illumination levels. Nonetheless, the shielded photosensor system allowed total light levels to drop about 30% below the design level at 12:30 and 3:30 pm; therefore its performance still must be considered suboptimal.

The P_{tl} photosensor, which measured task luminance, generally performed in a similar manner (simulation not shown) as the P_{ces} photosensor just described, with light levels dropping 25% below the target level at 12:30 and 3:30 pm. However, the P_{tl} photosensor caused somewhat greater variability in task illuminance than the P_{ces} photosensor due to

the confounding effects of semi-specular surfaces at the work plane. This can also be seen in Table 1 by comparing the values of σ_B for these two photosensors.

Sliding set-point systems

Computer simulation also was used to calculate the light levels on the task surface for systems employing the sliding set-point algorithm. Eqs. (18a) and (18b) were used for these simulations; values of M were determined by substituting the *average value* of B for each photosensor and drape condition for the right side of Eq. (17). Note that this method of determining M is equivalent to assuming that each system was calibrated under "average" daylight conditions.

Figure 4 shows the maintained light levels (drapes closed) for a system using the sliding set-point algorithm and controlled by the shielded ceiling-mounted photosensor, P_{css}. Light levels at the task surface were maintained at the target level to within better than 8%. From inspection of the σ_B data in Table 1, it is apparent that the deviations from the target light level were due only to the fact that the relationship between $S_D(t)$ and $I_D(t)$ was not exactly proportional, presumably because the relative distribution of daylight throughout the space was not exactly constant with time. The observed fluctuations from the target level are sufficiently small (at least compared to the ability of the human eye to detect such changes) that one can positively state that the P_{css} photosensor, when used in conjunction with a sliding set-point system, satisfactorily achieved the objective of equi-illumination.

Figure 5 shows the simulated performance of a sliding set-point system driven by the unshielded ceiling-mounted photosensor, P_{ce}, with the drapes closed. For the situation examined here (i.e., assuming, as before,

that the system was calibrated under average *drapes-closed* conditions),
this system performs as well as the previous one, providing sufficient
electric illumination throughout the day to meet the target level. This
considerable improvement in performance relative to the situation dep-
icted in Fig. 2 indicates that the sliding set-point algorithm enhances the
equi-illumination potential of both shielded and unshielded photosensors.
Nonetheless, as discussed below, the unshielded photosensor was found to
be considerably inferior to the photosensors that were shielded from
direct light from the window.

DISCUSSION

All the photosensors we tested were found to have B less than one.
This indicates that, if used with constant set-point systems, all of the
tested photosensors would allow total light levels at the task to drop
below the target design level for most daylight conditions. Even P_{tl}, the
photosensor with values of B closest to one, allowed total light levels to
drop as much as 25% below the target level (simulation not shown), with
other photosensors faring much worse.

To achieve the objective of equi-illumination at the task, we found it
necessary to assume the use of a novel photoelectric control system that
incorporates a sliding set-point control algorithm rather than the con-
ventional constant set-point. The system performance of a photosensor
that does not satisfy Eq. (13) can always be improved with the sliding set-
point algorithm because a sliding set-point system enables the user to
compensate for differences in the spatial distribution of daylight and
electric light relative to the task and sensor. Nonetheless, the t-
statistics in Table 1 indicate that it would be an oversimplification to sup-
pose that the sliding set-point algorithm eliminates the need to shield

the photosensor from direct window luminance. To show this, Student's t-statistic is used to test whether values of the fitted parameter B for the drapes-open and drapes-closed data sets for each photosensor can be distinguished statistically. (If the t-statistic for a photosensor is equal to 2, then the drapes-open and drapes-closed data sets may be considered statistically indistinguishable to a 95% confidence level; higher values of the t-statistic correspond to greater differences between the data sets.) Based on this statistic, only the shielded photosensors P_{ces} and P_{tl} (with t-statistics of 1.8 and 1.1, respectively) have statistically indistinguishable values of B for both drapes open and closed; therefore only these two photosensors have the same value of M for both conditions. The other photosensors, including the P_{ce} photosensor simulated in Fig. 5, require one value of M for drapes open and a different M for drapes closed. To appreciate the practical significance of this, the reader should realize that the value of M used in the simulation in Figs. 4 and 5 assumed that the system was calibrated under average drapes-closed conditions. If we had instead used a value of M to optimize performance (i.e., maintain equi-illumination) with drapes open, then light levels for the unshielded photosensor would have fallen below the target level under drapes-closed conditions. Our data show that only the P_{ces} and the P_{tl} photosensors had values of B that were insensitive to drape configuration, suggesting that even with a sliding set-point system, a control photosensor that is shielded from direct window luminance is better suited to equi-illuination purposes than an unbaffled sensor. From our results, we conclude that the objective of equi-illumination was achieved when either the P_{ces} or the P_{tl} photosensor was used in conjunction with a sliding set-point system.

CONCLUSION

This study has shown that the ability of a constant set-point system to achieve equi-illumination at a work surface is strongly influenced by photosensor location and configuration. None of the tested systems that used the constant set-point algorithm were able to maintain the target light level at all times, although shielding the photosensor from window luminance resulted in higher illumination levels with less variability. Our data indicate that the goal of equi-illumination can be achieved by using a sliding set-point algorithm, in conjunction with a photosensor that is shielded from direct window light. The data also suggest that the poor performance associated with unshielded photosensors can be greatly improved with a sliding set-point algorithm, although shielded photosensors were still found to be preferable. Although more research is required before it is possible to generalize, it would appear that the incorporation of a sliding set-point algorithm may considerably enhance the performance of tomorrow's lighting control systems.

ACKNOWLEDGEMENT

REFERENCES

1   D.R.G. Hunt and V.H.C. Crisp, "Lighting Controls: Their Current Use and Possible Improvement," *International Journal of Energy Research*, vol. 2, no. 4, pp. 343-374, 1978.

2   A. Levy, "Lighting Controls, Patterns of Lighting Consumption, and Energy Conservation," *IEEE Transactions on Industry Applications*, vol. IA-16, no. 3, pp. 419-427, 1980.

3   F. Rubinstein and M. Karayel, "The Measured Energy Savings from Two Lighting Control Strategies," *Conference Record of the IEEE Industry Applications Society Annual Meeting*, pp. 1342-1349, 1982.

4   V.H.C Crisp, "Energy Conservation in Buildings: A Preliminary Study of the Use of Automatic Daylight Control of Artificial Lighting," *Lighting Research & Technology*, vol. 9, no. 1, pp. 31-41, 1977.

TABLE 1

Photosensor	ALL DATA				DRAPES CLOSED				DRAPES OPEN				
	N^a	B^b	σ_B^c	r^d	N	B_{cl}	σ_B	r	N	B_{op}	σ_B	r	t-statistic^e
P_{ce}	21	0.19	0.013	0.84	15	0.17	0.005	0.98	6	0.28	0.03	0.69	5.3
P_{ces}	21	0.67	0.016	0.98	15	0.7	0.02	0.98	6	0.63	0.02	0.98	1.86
P_{tl}	20	0.78	0.03	0.95	14	0.82	0.03	0.97	6	0.75	0.06	0.85	1.1
P_{NE}	21	0.32	0.017	0.9	15	0.4	0.01	0.98	6	0.28	0.02	0.84	5.9
P_{SE}	21	0.72	0.035	0.92	15	0.65	0.03	0.96	6	0.84	0.07	0.81	3
P_{NW}	21	0.021	0.002	0.6	15	0.039	0.001	0.98	6	0.017	0.003	0.27	8.6

a Number of data points. Points for which $I_D(t) > 1.5\ I_{E_{max}}$ are excluded.

b Least-squares of $\dfrac{I_D}{I_{E_{max}}} = B\ \dfrac{S_D}{S_{E_{max}}}$.

c Uncertainty in B.

d Linear correlation co-efficient.

e Calculated from $\dfrac{B_{cl}-B_{op}}{\sigma_\delta}$, where σ_δ is the uncertainty of $B_{cl}-B_{op}$.

Table 1. Relationship between S_D and I_D for six photosensors under drapes open and closed conditions.

Electric
Power

| Photosensor Signal | → | Logic Circuit | Dimming Control Signal → | Dimming Unit |

Control Photosensor

Power
to Lighting
Circuit

Lighting
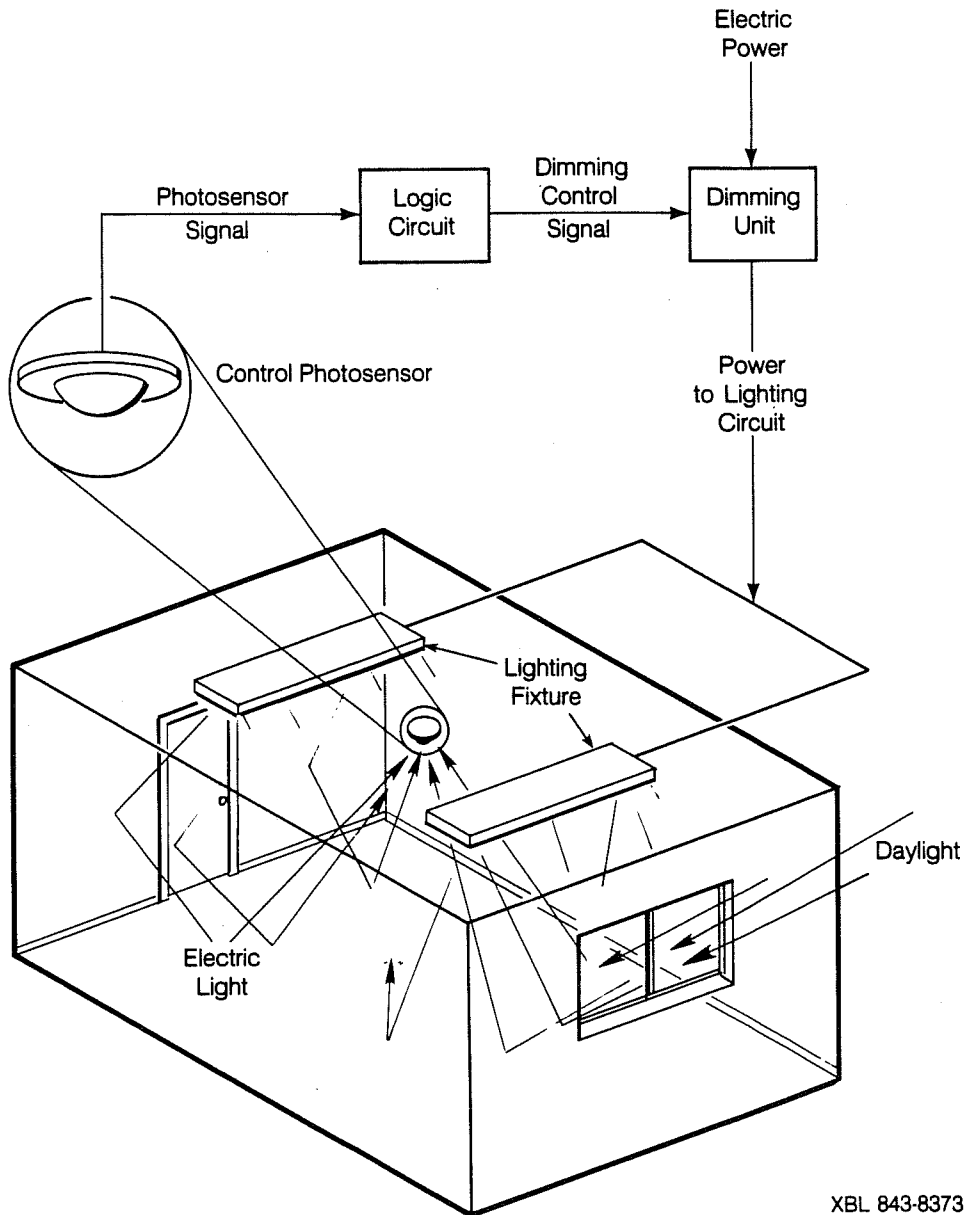Fixture

Daylight

Electric
Light

XBL 843-8373

Figure 1. Graphical representation showing the relationship between the components of a photo-electric dimming system in a typical building application. The ceiling-mounted control photosensor is sensitive to electric light within the space and incoming daylight.
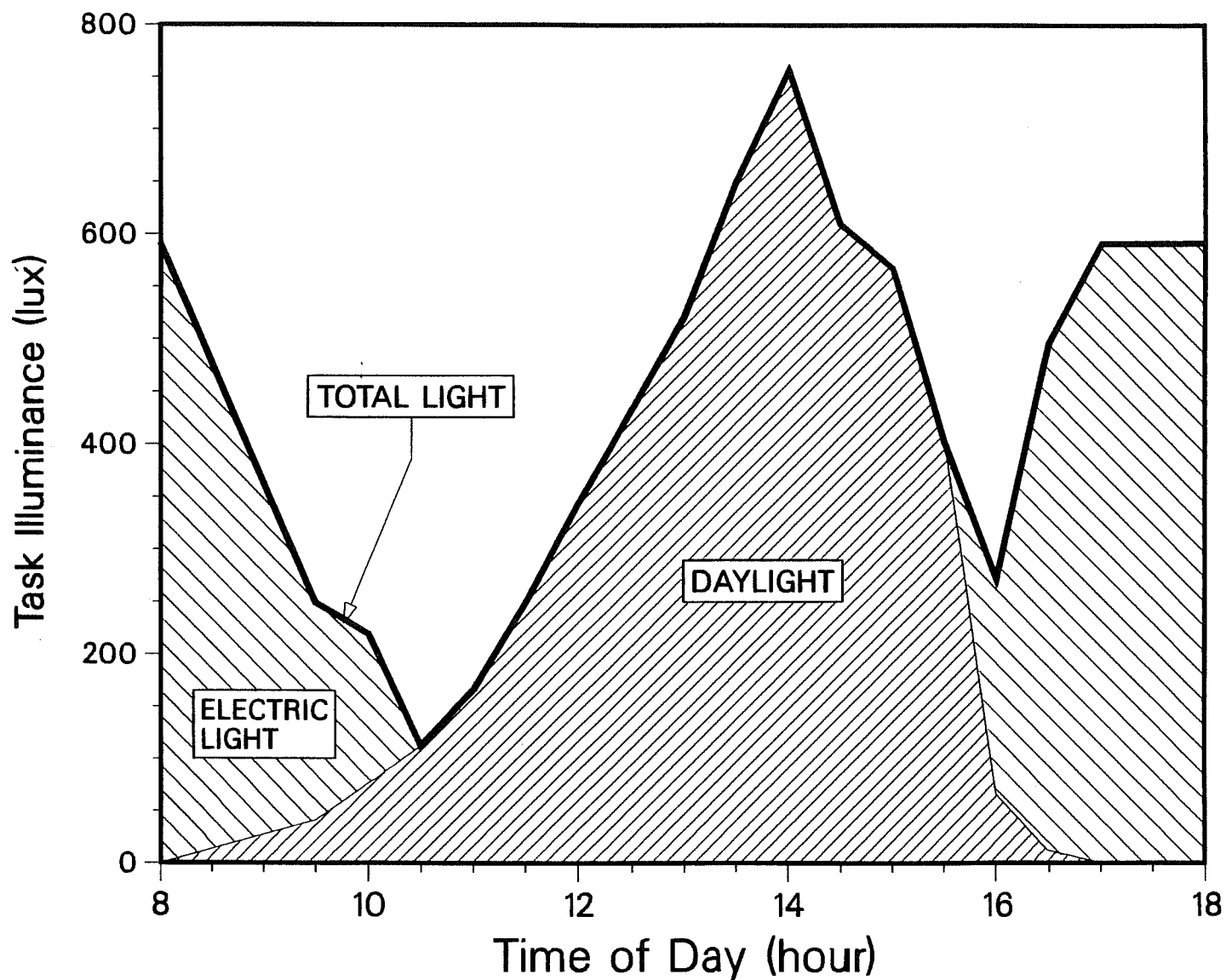
Figure 2. Total illumination on task surface for a constant set-point system driven by the unshielded photosensor P_{ce}. Shaded areas indicate relative contributions of daylight and electric light to the total maintained light level. Daylight conditions: Nov. 28, clear sky, southwest elevation, drapes closed.
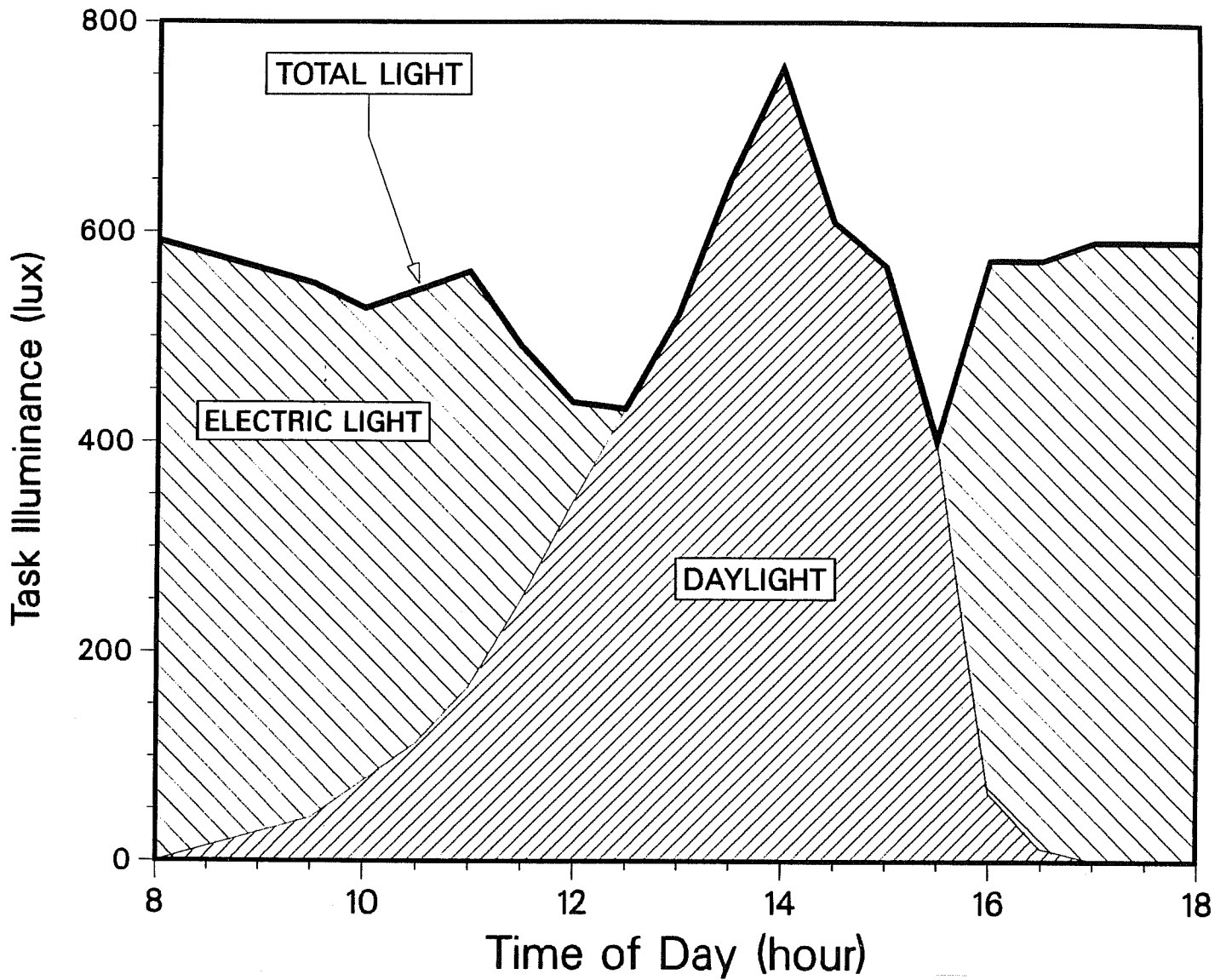
Figure 3. Total illumination on task surface for a constant set-point system driven by the unshielded photosensor P_{ces}. Shaded areas indicate relative contributions of daylight and electric light to the total maintained light level. Daylight conditions: Nov. 28, clear sky, southwest elevation, drapes closed.
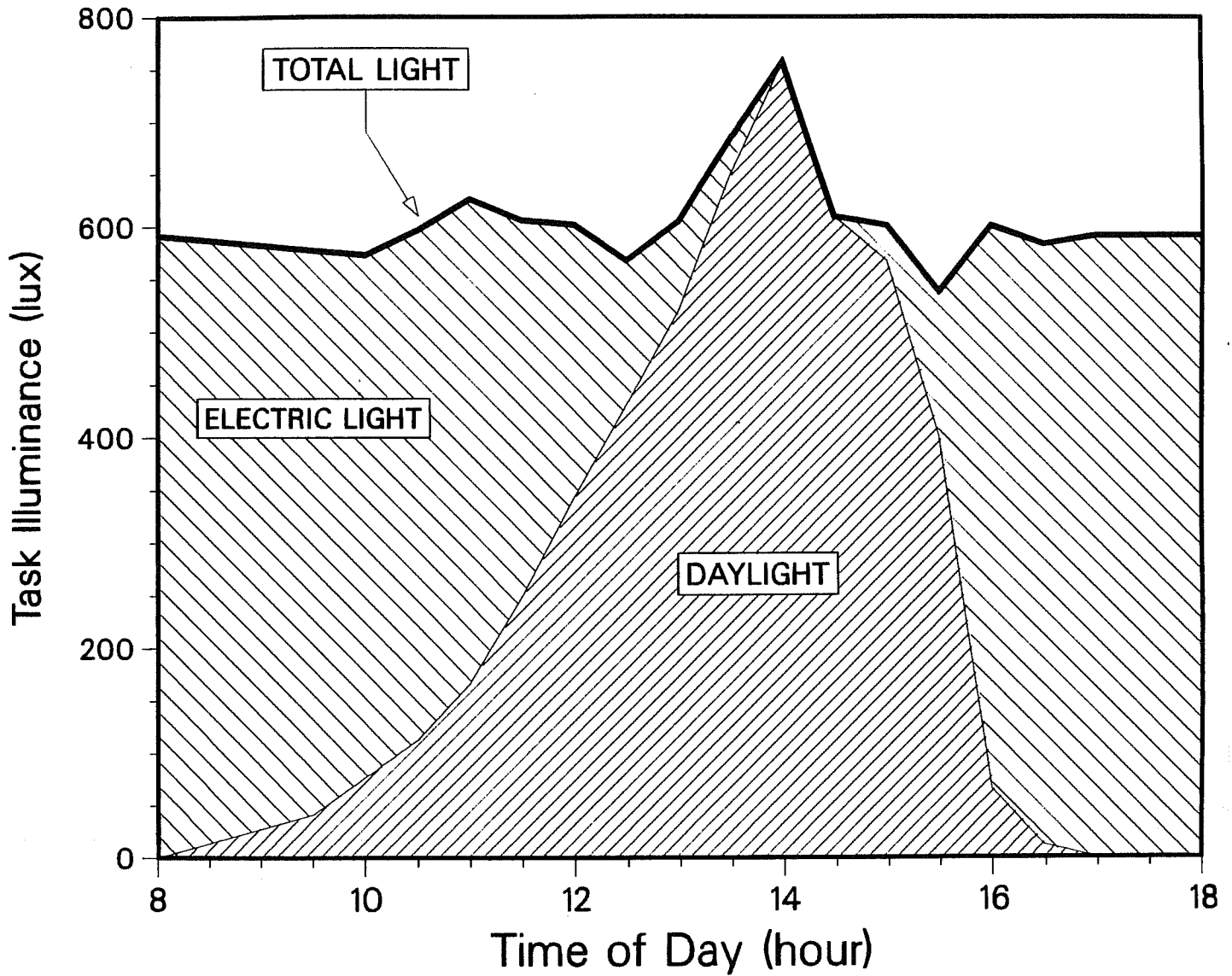
Figure 4. Total illumination on task surface for a sliding set-point system driven by the shielded photosensor P_{ces}. Shaded areas indicate relative contributions of daylight and electric light to the total maintained light level. Daylight conditions: Nov. 28, clear sky, southwest elevation, drapes closed.
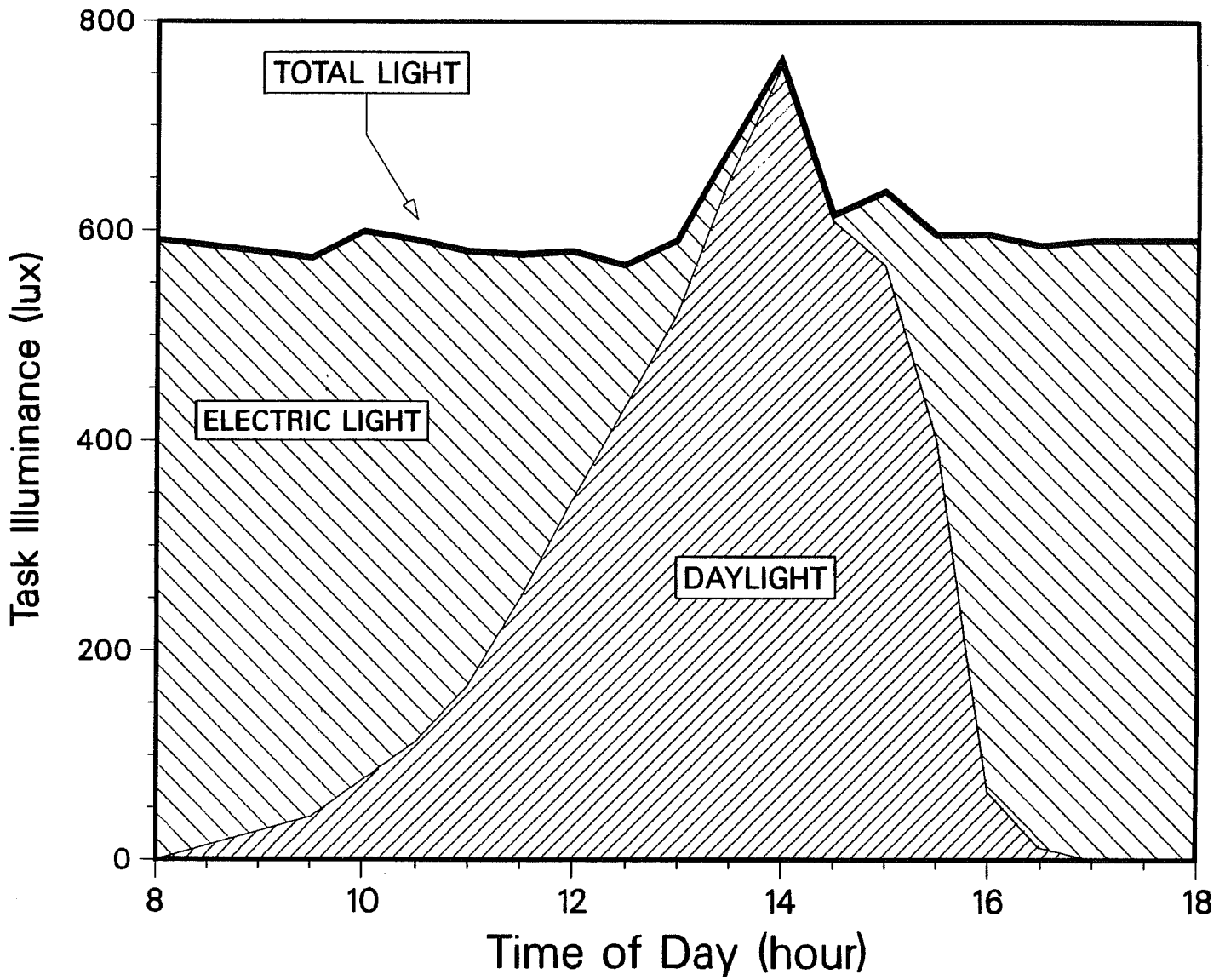
Figure 5. Total illumination on task surface for a sliding set-point system driven by the unshielded photosensor P_{ca}. Shaded areas indicate relative contributions of daylight and electric light to the total maintained light level. Daylight conditions: Nov. 28, clear sky, southwest elevation, drapes closed.